

A dopant-free polyelectrolyte Hole-transport Layer for High Efficiency and Stable Planar Perovskite Solar Cells

Wenxiao Zhang, Li Wan, Xiaodong Li, Yulei Wu, Sheng Fu, and Junfeng Fang*

Experimental Section:

Materials: The SnO₂ colloid precursor and 2, 2, 2-trifluoroethanol (99% +) was obtained from Alfa Aesar (tin (IV) oxide). CPTA (97%), N,N-dimethylformamide (DMF), and dimethyl sulfoxide (DMSO) were purchased from Sigma-Aldrich. Methylammonium iodide (MAI), PbI₂ and Spiro-OMeTAD were purchased from Xi'an Polymer Light Technology Corp. Poly [3-(4-carboxylbutyl)thiophene] (P3CT) was purchased from Rieke, America.

Fabrication of Perovskite Solar Cells: ITO glass was cleaned by sequentially washing with detergent, deionized (DI) water, acetone, and isopropanol (IPA). Before using, the cleaned substrate was dried with N₂ flow and then treated in O₂ plasma for 15 min. Then, the substrate was spin coated with a thin layer of SnO₂ nanoparticle film (1.875%) at 4000 rpm for 30 s, and annealed in ambient air at 150 °C for 30 min. The CPTA solution (3 mg/ml in NMP) was spin coated at 4000 rpm for 30 s followed by annealing at 140 °C for 10 min in a N₂ filled glovebox. Next, a perovskite precursor solution (1.45 M in a DMF/DMSO mixture with a 1:1 molar ratio of PbI₂ to MAI) was deposited on the ITO/SnO₂/CPTA substrate through spin-coating at 4800 rpm for 30 s with CB anti solvent treatment 8 s after the spin-coating began. Then the film was annealed at 60 °C for 1 min and then at 80 °C for 3 min. The P3CT-BN hole-transport solution containing 20 mg P3CT and 10.9 µl butylamine in 1.0 ml 2, 2, 2-trifluoroethanol was prepared after dissolving at 60 °C overnight. Then the P3CT-BN solution was diluted to 3 mg/ml then was spin-coated on the perovskite layer at 2000 rpm for 30 s. The Spiro-OMeTAD hole-transport solution was prepared by dissolved 72.3 mg Spiro-OMeTAD, 28.8 µl Tbp and 17.5 µl Li-TFSI (520 mg/ml in acetonitrile) in 1 ml chlorobenzene. The Spiro-OMeTAD layer was deposited on perovskite by spin-coating at 4000 rpm for 30 s, followed by deposition of an 80 nm patterned Au top electrode by thermal evaporation. All of the abovementioned solutions were filtered through a 0.45 µm polytetrafluoroethylene filter prior to use.

Characterization and Measurements:

Photocurrent density-voltage (*J-V*) curves were measured using Keithley 2440 sourcemeter controlled by computer under simulated AM1.5G spectrum (100 mW/cm²) with an Oriel So13A solar simulator.

The external quantum efficiency (EQE) measurement was conducted with a Newport quantum efficiency measurement system (ORIEL IQE 200TM) combined with a lock-in amplifier and a 150 W Xe lamp in ambient atmosphere. The light intensity at each wavelength was calibrated by a standard Si/Ge solar cell.

Electron spin resonance (ESR) spectra were analyzed by a Bruker-E500 spectrometer

Scanning electron microscope (SEM) images were acquired by using a field-emission scanning electron microscopy (Hitachi, S-4800) with an accelerating voltage of 10 kV. Atomic force microscopy (AFM, Dimension 3100V, Veeco, tapping mode) was applied to observe the film surface morphology.

The fourier transform infrared (FRIT) spectroscopy was characterized with a NICOLET 6700 (Thermo Fisher Scientific, USA) instrument.

Cyclic voltammetry (CV) measurements were carried out on a CHI 660e electrochemical analyzer with a three-electrode cell under nitrogen atmosphere in a deoxygenated anhydrous acetonitrile solution of tetra-n-butylammonium-hexa-fluorophosphate (0.1 M) under a nitrogen atmosphere. A platinum disk electrode, platinum-wire, and Ag/AgCl electrode were used as a working electrode, a counter electrode, and a reference electrode, respectively, with the polymer thin film for evaluation coated on the surface of platinum disk electrode. Ferrocene/ferrocenium (Fc/Fc⁺) was used as the internal standard (the energy level of Fc/Fc⁺ is -4.8 eV under vacuum).

X-ray photoelectron spectroscopy (XPS) and ultraviolet photoelectron spectroscopy (UPS) measurements were carried out using Kratos AXIS ULTRA DALD XPS/UPS system. XPS spectroscopy was collected to identify the overall surface composition using a monochromatic Al K α X-ray source (1486.6 eV). UPS measurement was conducted using a HeI (21.2 eV) discharge lamp operated at 20 mA, a pass energy of 5 eV, and a channel width of 25 meV.

X-ray diffractometer (XRD, Bruker AXS D8 Advance, Germany) equipped with Cu K α radiation ($\lambda = 0.154$ nm) was applied to analyze the crystallinity of perovskite film.

UV-vis absorption spectrum was recorded on a GS54T spectrophotometer (Shanghai Lengguang Technology Co., China).

Photoluminescence (PL) spectra was analyzed using a fluorescence spectrophotometer (F-4600, Hitachi

Ltd., Tokyo, Japan) with a 150 W Xe lamp with excitation wavelength at 466 nm.

Time-resolved photoluminescence (TRPL, LabRAM HR800, Horiba Jobin Yvon) decays were conducted with a 532 nm diode laser used as the excitation source.

EIS was measured under dark at a reverse potential of 0.8 V at frequencies ranging from 1.0 Hz to 1.0 MHz and the oscillation potential amplitudes are 20 mV using Solartron 1260A impedance analyzer.

The hole mobility (μ) was evaluated with the Mott–Gurney law, given by the equation: $J = 9\epsilon_0\epsilon_r\mu V^2 \exp(0.89\beta(V/L)^{0.5}) / (8L^3)$, where J stands for the current density, ϵ_0 the permittivity of free space, ϵ_r the relative permittivity of the medium (assuming that 3.4), V the effective voltage, L the thickness of the active layer, and β the field activation factor.

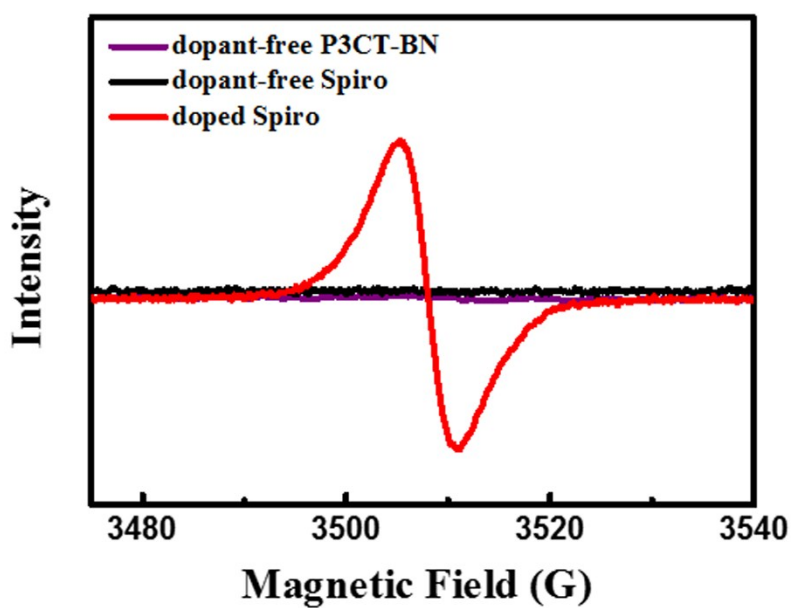


Fig. S1 Electron spin resonance (ESR) spectra of dopant-free P3CT-BN, dopant-free Spiro and Spiro with Li-TFSI and tBP dopants.

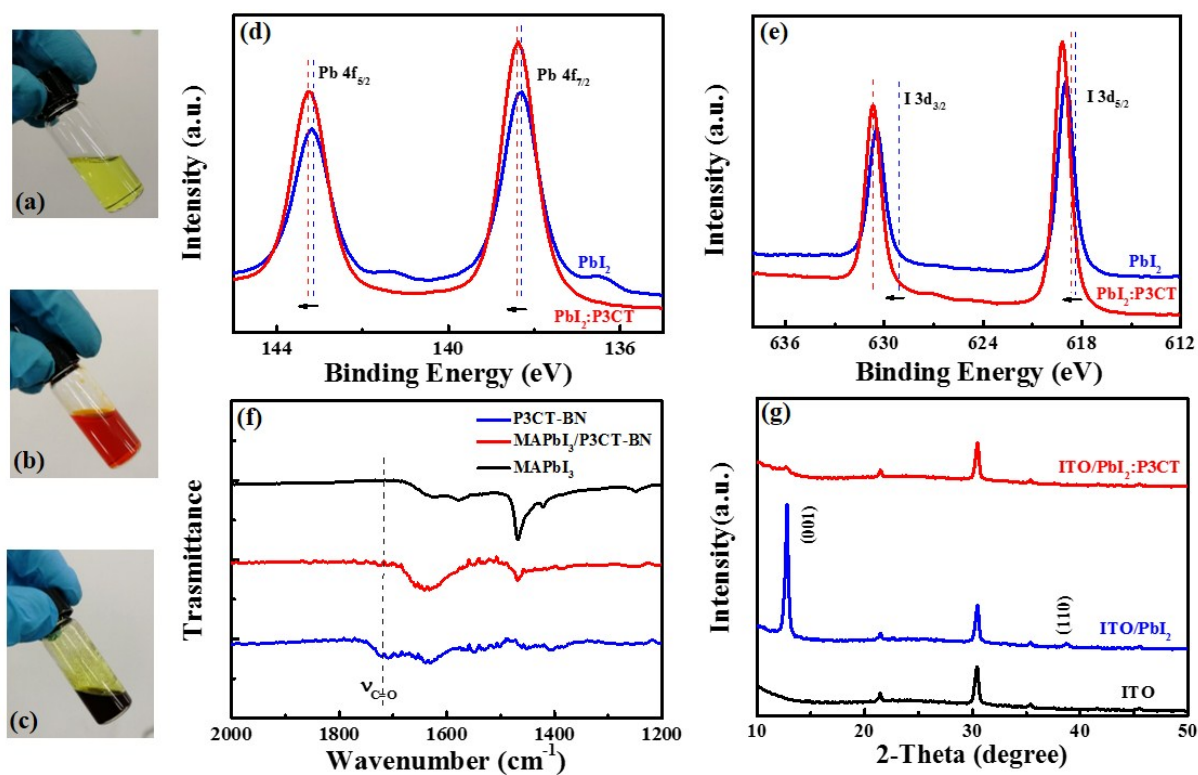


Fig. S2 (a-b) The graph of PbI_2 and P3CT dissolving in DMF solvent, respectively. (c) The graph of the mixture of PbI_2 and P3CT solution, showing the appearance of precipitation. High-resolution XPS of Pb 4f (d) and I 3d (e) core levels of ITO/ PbI_2 and ITO/ PbI_2 :P3CT film. (f) FTIR spectra of pristine MAPbI_3 film, P3CT-BN film and the MAPbI_3 /P3CT-BN bilayer film. (g) XRD patterns of ITO glass and the ITO glass, ITO/ PbI_2 and ITO/ PbI_2 :P3CT film.

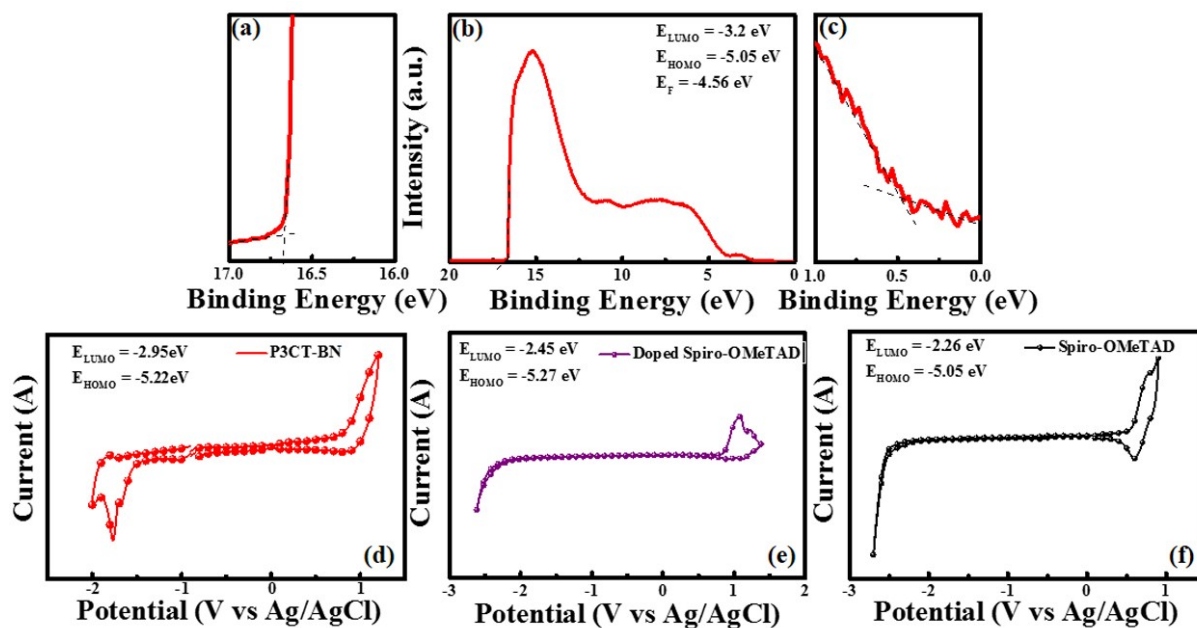


Fig. S3 (a-c) The full UPS spectra (b), secondary-electron cut-off (a), and valence-band region (c) of the P3CT-BN film coated on ITO substrate. (d-f) Cyclic voltammograms of P3CT-BN (d), doped Spiro-OMeTAD (e) and pristine Spiro-OMeTAD HTL (f).

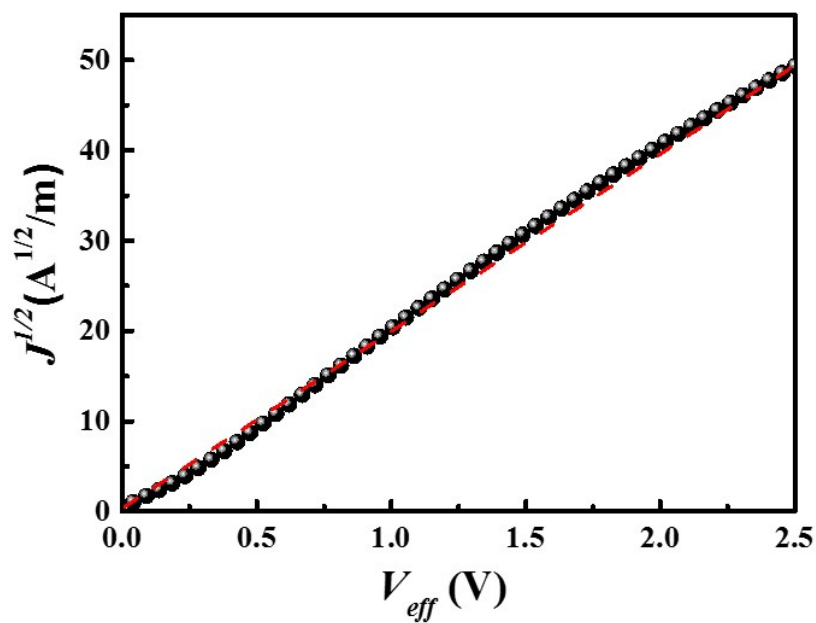


Fig. S4 J - V plots of the hole-only devices based on pristine Spiro HTM.

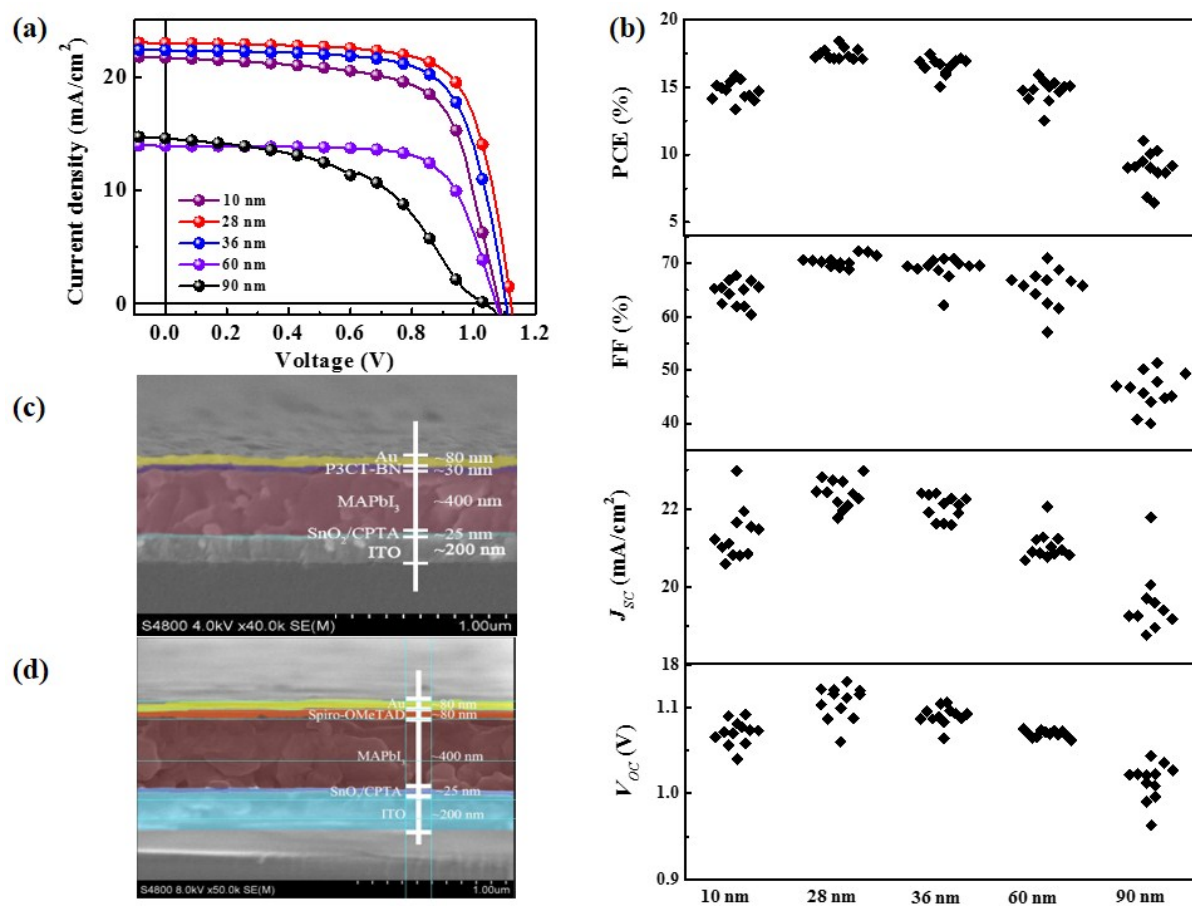


Fig S5 (a) J - V scans collected under AM 1.5 simulated sunlight for P3CT-BN with different thickness. (b) Statistical parameters of 12 devices based on P3CT-BN with different thickness. (c-d) The cross-section SEM image of the planar solar cells based on P3CT-BN and Spiro HTL, respectively.

Table S1 Detailed parameters of devices based on P3CT-BN HTL with different thickness.

P3CT-BN thickness (nm)	V_{oc} (V)	J_{sc} (mA/cm ²)	FF (%)	PCE (%)
10	1.08	21.65	67.7	15.8
28	1.12	22.73	72.2	18.4
36	1.10	22.35	10.6	17.4
60	1.07	20.86	71.0	15.89
90	1.03	21.77	44.0	11.04

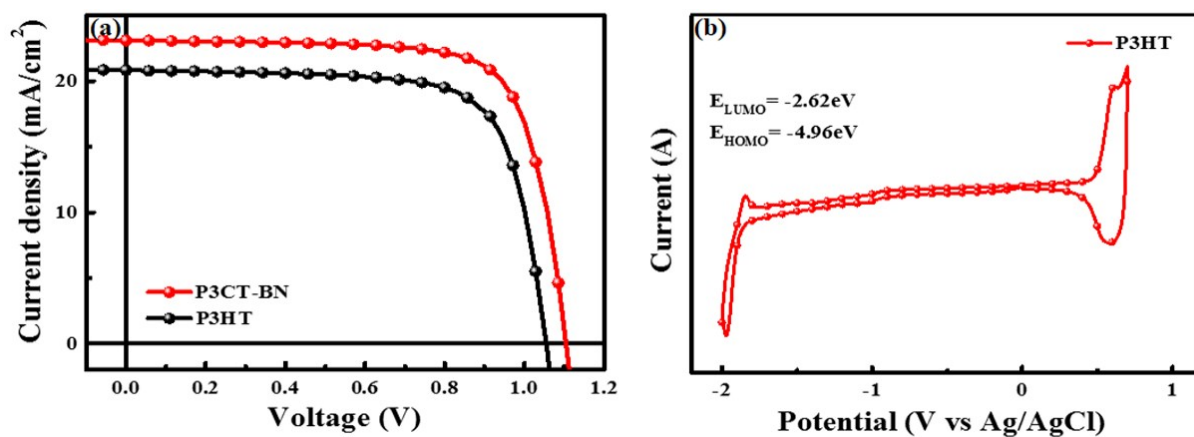


Fig. S6 (a) Best-performing J - V scans collected under AM 1.5G simulated sunlight for P3CT-BN and P3HT based solar cells. (b) Cyclic voltammograms of pristine P3HT.

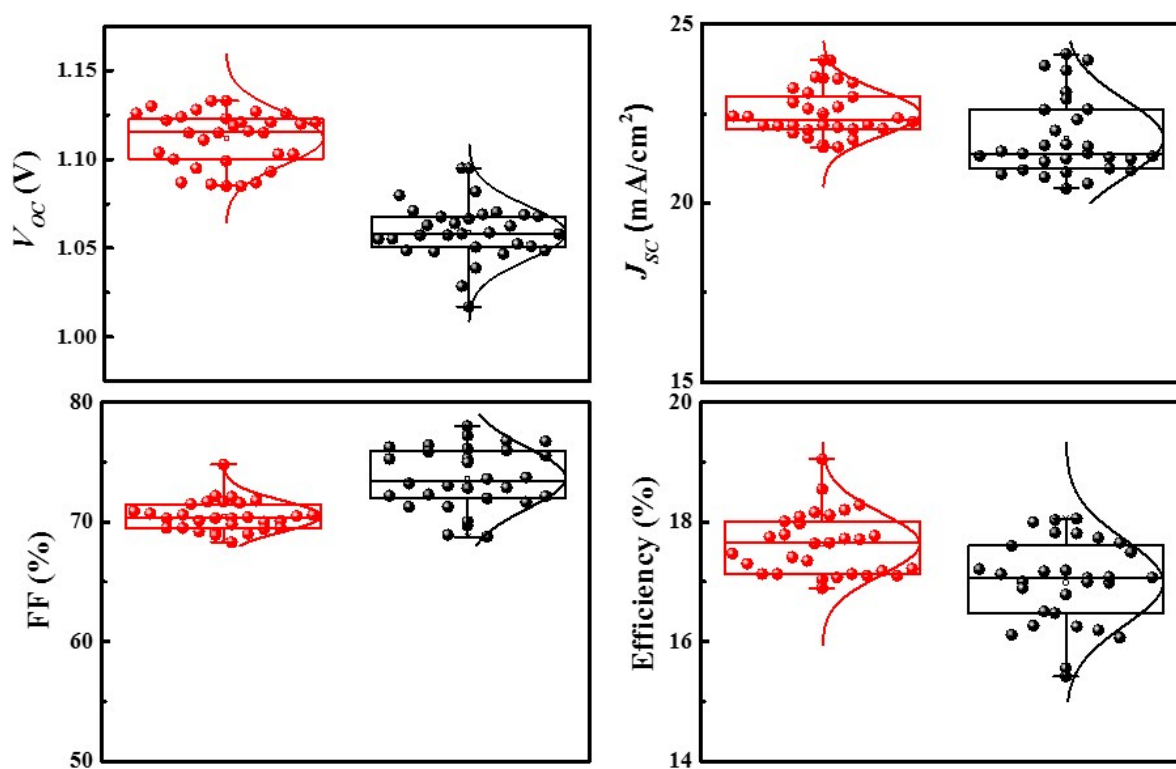


Fig. S7 Parameters of 30 devices based on P3CT-BN and Spiro HTL. (a-d) V_{oc} , J_{sc} , FF and PCE, respectively.